20231082

Investigations on the energy saving potential of X-by-wire chassis systems and advanced integrated control strategies

Marius Heydrich [1)] **Christopher Hamatschek** [1)] **Markus Gundlfinger** [2)] **Christian Eichhammer** [2)]
Claus Lechner [3)] **Christoph Fachbach** [3)] **Florian Büchner** [1)] **Valentin Ivanov** [1)]
Sebastian Gramstat [2)] **Eric Armengaud** [3,4)]

1) *University of Technology Ilmenau, Automotive Engineering Group, 98693 Ilmenau, Germany (marius.heydrich@tu-ilmenau.de)*
2) *AUDI AG, 85045 Ingolstadt Germany*
3) *AVL List GmbH, 8020 Graz, Austria*
4) *Armengaud Innovate GmbH, 8144 Haselsdorf-Tobelbad, Austria*

ABSTRACT: This paper describes real-world driving tests with a battery-electric sport utility vehicle equipped with innovative chassis actuators such as high-torque in-wheel machines and a hybrid brake-by-wire (BBW) system tailored specifically for electric vehicles. In addition, the vehicle incorporates a new E/E architecture and communication bus systems to integrate the new components into the global bus network. Integrated control functions are used to investigate the potential of the new by-wire actuators to improve energy efficiency. To this end, the vehicle is tested in comparison with a series vehicle. The focus of the presented experiments is on the energy saving potential through integrated control of the subsystems for different functions such as regenerative wheel slip control or torque blending. At the end, a comparison is made between the baseline vehicle with standard centralized powertrain and friction braking system and the demonstrator with the adapted actuators to show the advantages in terms of overall efficiency and energy consumption.

KEY WORDS: **Brake-by-wire, In-Wheel Propulsion, Energy Efficiency, Battery-electric Vehicle, Integrated Vehicle Control**

1. INTRODUCTION

A rapidly growing market and climate-friendly policies are accelerating the development of third-generation electric vehicles. In 2022, the combined share of battery electric vehicles (BEVs) and plug-in hybrids (PHEVs) in global light-duty car sales reached 13%. In absolute terms, sales of BEVs and PHEVs increased by an average of 56.7% annually from 2013 to 2022. The share of sales reached double digits for the first time. (1)

Electric vehicles outperform conventional vehicles with internal combustion engine in several aspects, including emissions, simplicity, comfort, and efficiency as investigated in (2). Additionally, there are significant opportunities in controlling vehicle dynamics through faster electric motor responses and more degrees of freedom in vehicle automation. However, these aspects still face major challenges. In this context, some examples are: limited range, long charging times, battery costs, and higher overall vehicle mass (2). Further, aspects of life cycle assessment and life cycle emissions have increasingly come into focus in recent years. (3)(4).

To improve the next generation of battery electric vehicles and further increase user acceptance, the European project "Electric Vehicle Components for 1000km daily trips" (EVC1000) was launched, see <https:\\evc1000.eu\en>. Taking into account the advantages of new chassis components such as in-wheel propulsion and brake-by-wire, as well as other aspects such as function integration, the project aimed to develop brand-independent chassis components for the above-mentioned requirements. Therefore, two demonstration vehicles are built, equipped with the developed components and tested for vehicle performance and efficiency to show the feasibility of EVs for daily long-distance trips up to 1000 km with a maximum of 90 minutes charging time, e.g. for vacation trips.

This article describes the real-world experiments on public roads under different conditions with one of these demonstration vehicles compared to the same vehicle type in series state. In the following sections, the design of the vehicle, the development of the control strategy and the test plan are described. At the end, it is shown that the new components in combination with integrated chassis control can reduce energy consumption compared with the reference baseline vehicle and .

2. VEHICLE DEMONSTRATORS

2.1 Test vehicles

Two sport utility vehicles are used as test objects. One is in series production condition ("baseline"), i.e. no technical modifications have been made to the vehicle. This applies in particular to the original powertrain, which is based on one asynchronous machine (ASM) per axle to enable electric all-wheel

drive with an output of up to 300 kW in boost mode, as well as the original brake-by-wire system. To increase driving torque and adjust wheel speeds during cornering maneuvers, the electric machines are connected to a planetary gearbox and a single-stage gear with integrated differential, each with a gear ratio of 9.205 (front) and 9.083 (rear) respectively. (5) Relevant technical data for the drivetrain is given in Table 1.

Through a bus gateway installed in the vehicle, access to the vehicle's FlexRay and CAN channels is granted. However, the original vehicle was further equipped with additional sensors and measuring unit for extensive research in different areas as exemplary presented in (6), e.g. pyrometers for detection of the brake disc temperatures, pressure sensors on the brake calipers and a high-precision, dual-antenna GPS system with inertial measuring unit (IMU) were installed. Through a data acquisition (DAQ) unit *cRIO* from National instruments it is possible to log the data at fixed sample rate of 100Hz in one measurement file. An overview of the systems is given in Fig. 1.

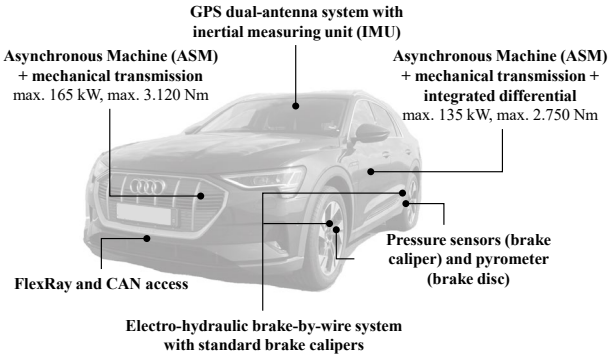

Fig. 1: Baseline vehicle with measurement equipment

In contrast to this vehicle, the EVC1000 demonstrator (Fig. 2) features a new e-axle concept that includes a high-torque in-wheel drive based on permanent magnet synchronous machines (PMSMs) and a dual inverter with silicon carbide (SiC)-based power stages. The use of two identical inverters with central control logic is advantageous in terms of packaging, hardware sharing and accurate timing synchronism, which is essential for a decentralized drivetrain architecture. (6)

The original brake-by-wire system has been replaced by a hybrid one with the original calipers on the front axle combined with electrohydraulic actuators, while new electromechanical sliding calipers are used on the rear axle. The latter are advantageous because their higher dynamics enable faster control for cooperative functions between friction brakes and the regenerative braking system, e.g. (brake) torque blending.

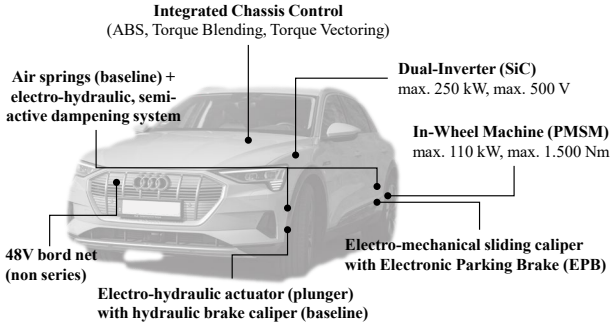

Fig. 2: Modified vehicle demonstrator and subcomponents

Table 1 Technical data of the vehicles

Parameter	Unit	baseline	modified
Vehicle total mass	[kg]	2565	2513
Maximum vehicle speed	[km/h]	200	165
Drivetrain topology		AWD	RWD
Electric machine type		ASM	PMSM
Drive torque (front axle)			
- nominal value	[Nm]	2200	-
- peak value	[Nm]	2750	-
Drive torque (rear axle)			
- nominal value	[Nm]	2800	1300
- peak value	[Nm]	3120	3000
Electrical drive power			
- nominal value	[kW]	165	130
- peak value	[kW]	300	220
Tires		255/50 R20 109Y	
Dynamic tire radius	[mm]	371	

In addition, the demonstrator features an electrohydraulic damping system designed to improve the vehicle's ride comfort and lateral stability. (6) However, these systems are not relevant in the context of this publication and will therefore not be discussed in the following sections.

Like the baseline vehicle, the EVC1000 demonstrator has access to several signals. First, it also has access to some of the original ECUs and is equipped with the identical GPS system and pyrometers as in the baseline vehicle to allow comparative studies between the two. Logging is done using a SCALEXIO AutoBox from dSPACE, which stores the newly developed integrated chassis controller and also serves as a real-time controller. This controller is described next.

2.2. Control design

Fully electric vehicles offer great potential for controlling vehicle dynamics. Combined with intelligent functions, the corresponding controllers can act independently of the driver and

a higher degree of vehicle automation is possible. Especially for energy efficiency, a defensive and predictive driving style is advantageous. In addition, due to the technical adaptations already mentioned, one or more new control units are required to restore the basic driving functionalities. In the present case, this is done with the integrated chassis controller outlined in Fig. 3. It contains various function blocks for generating traction/braking torque in response to driver demand, continuous wheel slip, and torque blending control. Some of the functions have already been presented in earlier publications by the authors (8)-(10). The outputs are forwarded to the subsystem control units, where low-level controllers convert the demands into actuator signals.

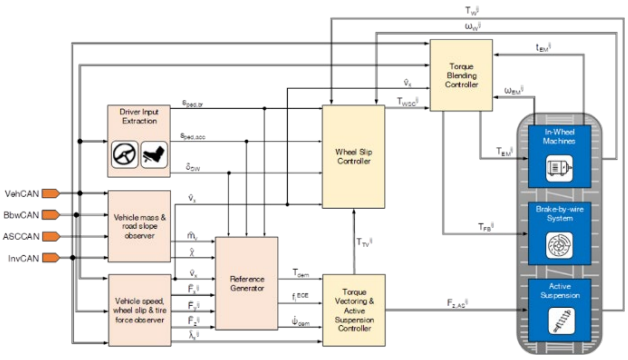

Fig. 3: Block scheme of the internal controller

For vehicle efficiency, the combined operation of regenerative and friction braking systems is essential to increase overall range and thus user acceptance. This function is called "(brake) torque blending" and aims to recover kinetic energy during braking by the electric machines, which are switched to generator mode for this purpose. This process is called "(energy) recuperation" and has a remarkable impact on efficiency, being responsible for 30% of the total vehicle range of the series vehicle under consideration. (11) In addition, the intelligent control and distribution of electric torque enables various functions.

The baseline vehicle has four different driving modes, namely "sailing" (default), "one-pedal driving I + II" and "automatic". In each mode, there is a different recuperation potential during the push mode. There is also a cleaning function for the friction brake. For this purpose, recuperation is suppressed for a certain amount of energy. This function is reactivated every 24 hours to wipe off water droplets or remove possible corrosion from the wheel brakes (4) to ensure optimal braking performance and to stabilize the friction coefficient over long time.

In the following experiments, the focus lies on the benchmark and optimization of the torque blending to improve energy recuperation and thereby vehicle range, so it is explained more in detail. Torque blending is the intelligent distribution of the total brake torque (T_{tot}) to the regerative torque (T_{rb}) and friction brake torque (T_{fb}). The factor α is the blending factor and T_{wsc} is the torque demand from the wheel slip controller (see Fig. 3).

$$T_{rb} = \text{sat}[\alpha T_{wsc}]_0^{T_{em,max}}$$
$$T_{fb} = T_{wsc} - T_{rb} \quad (1)$$

Generally, two options of blending are available: in parallel mode ($0 < \alpha < 1$), the regenerative torque is not fully used and the friction brakes are applied in every braking manoeuver. Thus, the full potential is not used. More common is the serial mode, whereby the blending factor is initially set to $\alpha = 1$, so the friction brakes are activated only in case the torque demand exceeds the maximum available regenerative torque ($T_{em,max}$) or for safety reasons (e.g., intervention of Electronic Stability (ESC) or Antilock Brake System (ABS) Control). There are several studies on the different strategies, but they are out of the scope of this article and therefore will not be discussed further. In the present investigations only serial blending is used to cover as many braking maneuvers as possible with the regenerative braking system alone, since (12) already showed good results for the present setup.

3. REAL-WORLD EFFICIENCY

3.1 Methodology

The real-world experiments were conducted using a driving cycle developed by Technische Universität Ilmenau (TUIL). Its development and execution takes into account EU Regulation 2016/427 for Real Driving Emissions (RDE) tests. Therefore, the cycle includes one-third driving in urban scenarios, on rural roads and on highways. Even though the route was not designed for the intended purpose, its topography makes it interesting for studies on efficiency, as a maximum altitude difference of 300 m is reached. Fig. 4 shows the route based on the GPS signals of both vehicles to prove that both were driven in the same cycle.

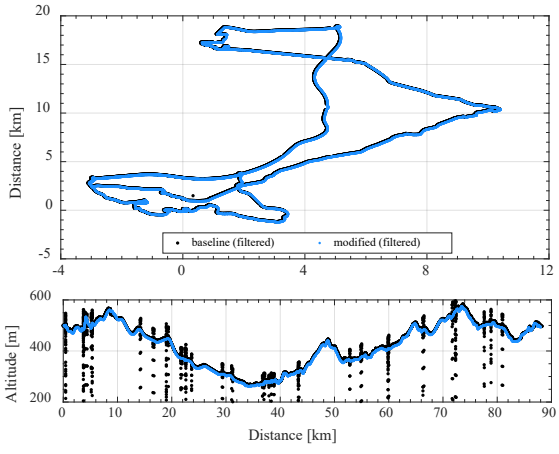

Fig. 4: Driving cycle of TUIL with elevation profile

The GPS signal was filtered with a fifth-order Savitzky-Golay filter because there were several short-term GPS interruptions during the test run due to structural conditions (tunnels, bridges, houses, etc.). The permanent signal losses are shown in the graph below with dashed values. The modified vehicle used the vehicle's original GPS module and signals. This provided somewhat more stable values, but was also strongly influenced by the structural conditions, so that filtering was also performed here, see Fig. 4.

In order to evaluate the experiments objectively and reliably, both vehicles run the cycle simultaneously in collone mode. In addition, some other limits were defined, namely:

a. traction batteries had a starting SoC of about 80%.
b. Both vehicles were equipped with winter tires of the same size, see Table 1. The tire pressure was adjusted to the manufacturer's specifications.
c. The air conditioning was set to 21°C automatic climate control in "eco" mode.

All experiments were performed only under dry, windless weather conditions. Special environmental conditions such as snow or rain were therefore not considered.

For the tests, the baseline vehicle uses the "sailing" mode, as this most closely corresponds to the operating behavior of the modified vehicle. In previous tests, a significant difference was found between the sailing mode and the one-pedal driving and the cleaning function in terms of frictional energy. (5) Therefore, the cleaning procedure was performed before the tests. The vehicle was then parked to cool the brake discs before the tests began.

Special attention was paid to an identical driving style of both drivers to meet RDE compliance requirements. Since there were no significant influences of the drivers over several test cycles, a single selected test run is discussed. Although the test drivers were not professionals, they have a wealth of experience and a high level of driving experience. Since the driver inputs and vehicle dynamics in particular (see Fig. 5 to Fig. 6) are comparable, there are no complaints at this point regarding the comparability of the tests. For mathematical verification, a linear regression of the vehicle speed was performed (see Fig. 5), which had a coverage of > 95%.

The g-g diagram in Fig. 6 proves that there were no sudden strong braking maneuvers in the cycles. This is important because in most cases blending is subject to maximum deceleration constraints, so gentle braking is strictly desirable.

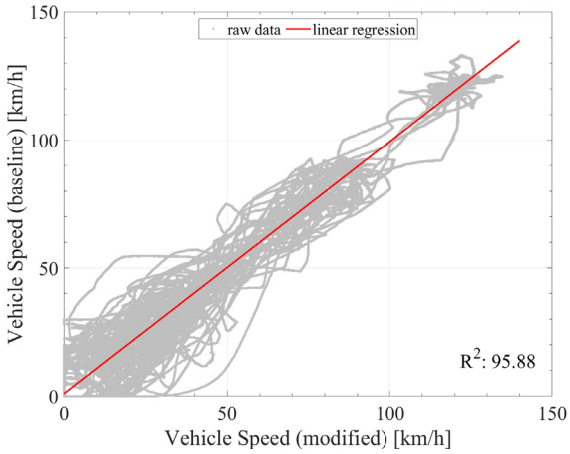

Fig. 5: Regression of vehicle speed signal during the cycle

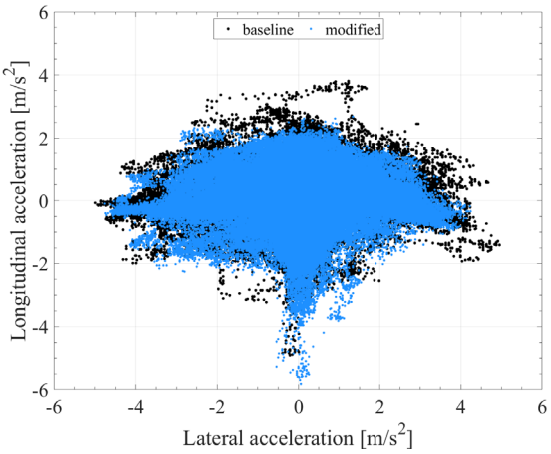

Fig. 6: g-g-diagram during cycle one

In the next section, the experimental results are discussed in detail. Since this article focuses mainly on brake blending and energy recovery, only the most important diagrams are selected.

As mentioned earlier, energy recuperation has a remarkable impact on the range of electric vehicles, as proper tuning can recover large amounts of kinetic energy, which can then recharge the traction battery and provide more electrical energy for longer trips. To evaluate the rides in this way, state of charge (SOC) is a commonly used indicator. It describes the remaining capacity of the traction battery relative to its total capacity that can be used for driving. Fig. 7 shows the SOC signal for both vehicles. Since it cannot be ensured that the vehicles start with identical SOC values, the signals were normalized to the start value. This gives the relative change. It can be seen that the baseline vehicle has a lower final value than the modified vehicle when the absolute difference between the starting and final values is considered. An explanation for this can be found directly in Fig. 7, as the modified vehicle has a lower decrease in the SOC signal in two notable sections between 9 and 30 km and between 66 and 70 km.

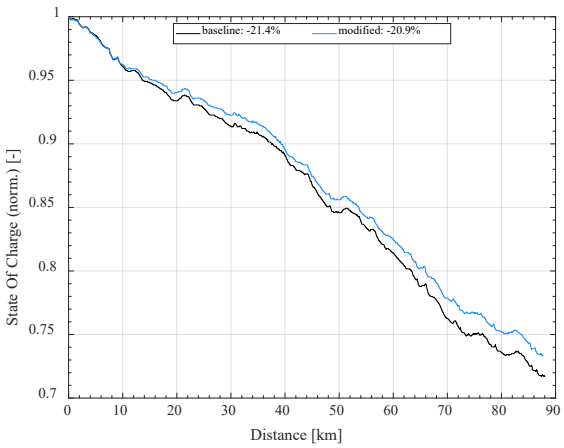

Fig. 7: State of Charge during one cycle

Based on Fig. 8, energy recovery is higher when driving on the highway ($v \geq 100$ km/h). This is due to the fact that the brake is usually applied gently on highways, since the bigger distance from the traffic ahead allows the ego vehicle to slow down at a lower deceleration. At lower deceleration, the pitch of the vehicle body is less, so the transfer of the dynamic wheel loads is smaller, allowing more braking force to be applied to the rear axle. This is of course advantageous for the modified vehicle, as it has electric rear-wheel drive only. Medially, the amount of recovered power lies at approx. 35.66 kW in this area. Even, if the maximum of 190 kW, which is nearly the full power of the in-wheel machines (see Table 1), seems to be reached on "country road", it relates to the highway section in reality. The classification is based on the vehicle speed and during the manoeuver, the vehicle felt below the threshold and was therefore classified in this way.

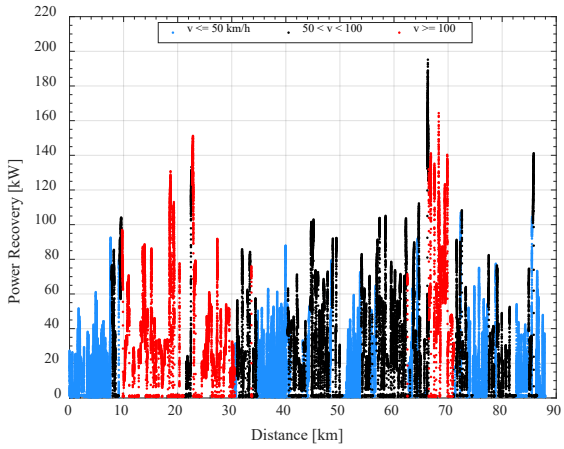

Fig. 8: Relation between vehicle speed and electrical power

To prove the previous assumption, Fig. 9 shows the relation between the longitudinal acceleration and the driving speed. There it can be seen that the baseline vehicle covers most of the braking maneuvers purely electrically. Only at speeds below 10 km/h is the friction brake also used until the regenerative braking system becomes inactive below 6 km/h. This is due to the internal blending strategy of the baseline vehicle, which gives priority to purely electric braking up to 0.3 g of the total braking torque demand. (13) Since there are almost no deceleration values above this threshold, there is a high percentage of purely electric braking due to RDE compliance while driving.

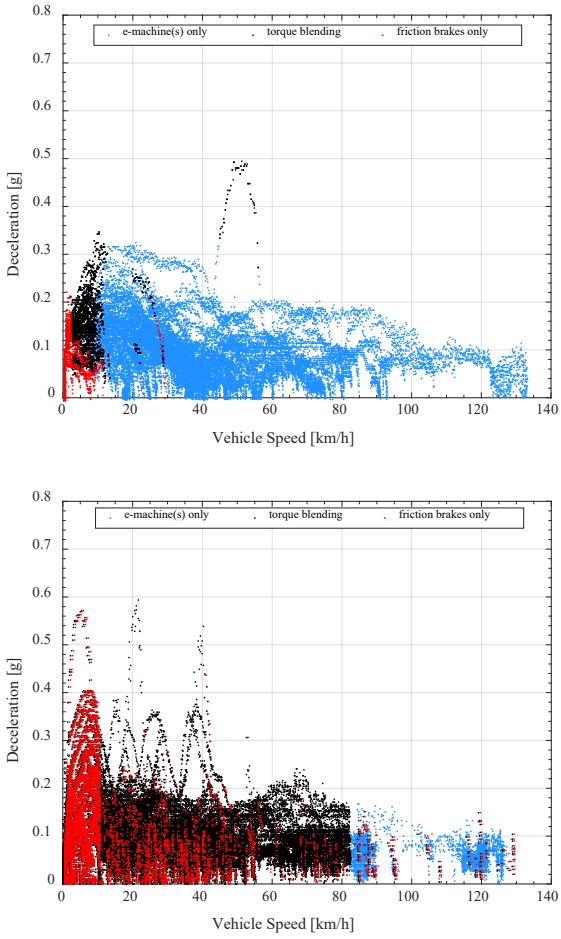

Fig. 9: Contribution of the friction and regenerative brake system for baseline (upper plot) and modified (lower plot) vehicle

In contrast, the modified vehicle shows three more or less sharply separated areas with only a small percentage where deceleration is purely electrical compared directly to the baseline vehicle. As mentioned earlier, this is the case at speeds above 80 km/h. Furthermore, the medium speed range is mainly covered by torque blending, while at lower speeds below 10 km/h the friction brakes must always be used, which is comparable to the baseline vehilcle and moreover a limitation due to the implemented blending controller, which takes into account the efficiency maps of the in-wheel machines. It is worth noting that

the implemented blending is an experimental approach that has not yet been optimized through extensive iterations. Accordingly, it is noteworthy that despite the fact that the controller has not yet been sufficiently tuned, the first improvements in terms of energy consumption have already been observed, see Fig. 7. This can be explained by the new drive system with fewer mechanical gear parts and synchronous instead of asynchronous electric machines. The latter require some of the consumed energy to generate the magnetic field in the stator, while the in-wheel machines use permanent magnets for this purpose. Therefore, PMSMs have a higher overall energy efficiency. Another important point is the thermal management of the electric machines, but since the investigations do not focus on this, it is only mentioned here for the sake of completeness.

In a next step, the experimental data were evaluated with an energetic approach. Therefore, the specific braking energy is introduced as follows where E_{br} and E_{kin} are the braking and kinetic energy amounts, T_{fb} and T_{rb} are again the torques of the friction and the regenerative brake system, and T_{act} is either the amount of the friction or the regenerative brake system to be able to investigate the systems separately.

$$E_{br}\,[\mathrm{kJ}] = E_{kin}\frac{T_{act}}{T_{fb}+T_{rb}} = \frac{m_v v_v^2}{2000}\frac{T_{act}}{T_{fb}+T_{rb}} \qquad (2)$$

The calculation considers, that E_{br} is only updated, when the brake pedal is pressed. In Fig. 10, the cumulative signal is plotted. It can be seen that there is a big difference between the two vehicles: For the baseline vehicle, the power of the regenerative braking system (RB) is much higher than for the friction braking system (FB). This fits with the results in Fig. 9. For the modified vehicle, the overall values are higher, but the difference between the two braking systems is smaller than before. This means that more energy is converted to heat in the friction brake system.

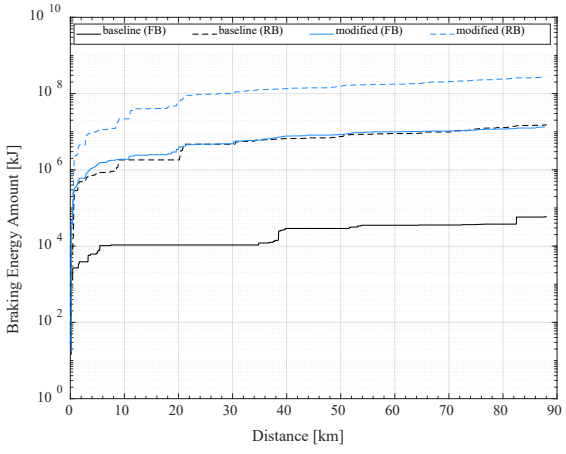

Fig. 10: Cumulated Amounts of Braking Energy

Summarizing the results so far, it is clear that the in-wheel machines have a high potential in terms of energy efficiency, but that some advantages are not fully exploited, so that the authors state that further research in this direction is necessary and intended, e.g., optimization of the brake force distribution and, above all, optimized tuning of the brake blending approach.

Looking at the data from Fig. 11, a high ratio of the braking energy is allocated to the friction brakes, converting kinetic into thermal energy. This indicates a higher heating power and leads to the conclusion that the temperature of the brake disc must increase proportionally. Fig. 10 shows the change of brake disc temperature at the front and rear left corners in relation to their start values.

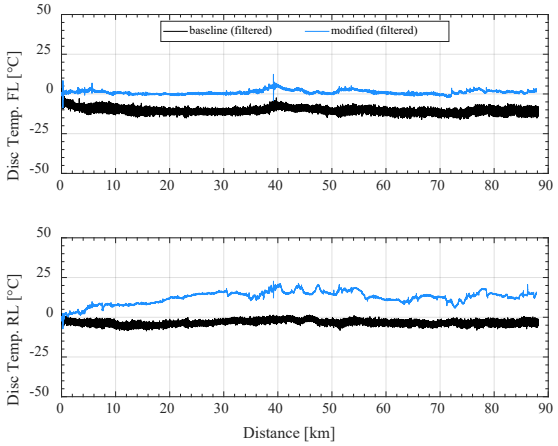

Fig. 11: Brake disc temperatures for the FL and RL corner

Due to the limited use of the friction brake, the temperatures at the baseline vehicle are almost constant for both axles. The only deviation is the higher initial value, due to the fact, that the vehicle was parked in a garage before the tests, whichs temperature was higher than the ambient temperature at the test start. Nevertheless, the curve is quite smooth. The disc temperature on the front brakes of the modified vehicle is noteworthy, as it also shows a fairly smooth curve, which is only slightly increasing. In the end, thee is only a remaining difference of 9.2 °C. In contrast, the rear axle discs show a significant increase in temperature. This underscores the fact that the brake blending controller is not yet optimally tuned and thus shows that there is still room for optimization in order to further exploit the positive energy-saving effects already achieved. The only noticeable feature is the obviously low cooling effect on the brake discs. This is due to the corners' architecture. The brake disc of the modified vehicle is completely enclosed by the stator of the in-wheel machine, so that less heat convection is possible. The baseline vehicle does not exhibit this behavior because its brakes are not enclosed. In addition, special air baffles

provide optimized airflow to the brake discs to increase heat exchange with the environment. This makes it possible to keep the temperature almost constant. Due to these air baffles, the temperature change at the front axle of the modified vehicle is also lower.

In addition to the indicators already mentioned, it is also interesting to examine the energy demand for driving, as overcoming driving resistance is the largest consumer of the electrical energy stored in the traction battery. It is calculated as poduct of the electric machines' torque (T_{em}) applied to the wheels and the wheel speeds (ω_w).

$$P_{dr}\,[\mathrm{kW}] = \frac{T_{em}\,\omega_w}{1000} \tag{3}$$

Fig. 12 shows the cumulative quantity for both vehicles. It can be seen that the drive energy demand for both vehicles is higher than the regenerative braking energy from Fig. 10, which is logical considering the decreasing state of charge in Fig. 7. However, the signals are very similar to each other due to the drivers, see Fig. 5 and Fig. 6.

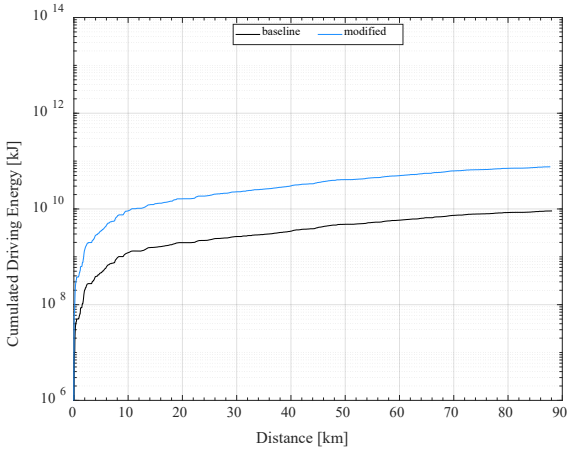

Fig. 12: Cumulated driving energy

Nevertheless, the energy demand of the modified vehicle is almost ten times higher compared to the baseline vehicle. This is related to the topology. While the baseline e-tron can accelerate with all-wheel drive, the modified e-tron is just able to use the in-wheel machines on the rear axle. Since the curb weight of both vehicle is nearly the same (see Table 1), more power is needed by the in-wheel machines to accelerate the vehicle or to overcome slopes at constant speed. In case of driving on flat road, the energy demand is remarkably lower. Another reason is the collone driving. While the vehicle ahead sets the target speed, the second vehicle must follow, which requires more acceleration. Therefore the power demand increases.

More common and more valuable for the customer is neither the driving energy nor the SOC change, as mentioned before, but the consumption of electrical energy. This value can be derived from the data. The most accurate way for calculation is given by the signals of the traction battery's voltage (U_{batt}) and current (I_{batt}).

$$E_{el}\,[\mathrm{kWh}] = \frac{U_{batt}\,I_{batt}}{3.6\times10^{6}} \tag{4}$$

The parameters are taken directly from the battery management system (BMS). In the modified vehicle, there is access to the battery CAN, but not in the baseline vehicle. Therefore, the state of charge data is used instead. Equation (5) gives the formula for the calculation, where t_0 and t_{end} are the time at the start and end of the driving cycle, respectively, and C_{tb} is the maximum capacity of the traction battery. In case of the target vehicle, the traction battery stores 83.6 kWh of usable electrical energy. (7)

$$E_{el}^{SOC}\,[\mathrm{kWh}] = \frac{\mathrm{SOC}(t_{end}) - \mathrm{SOC}(t_0)}{100}\,C_{tb} \tag{5}$$

Since the energy consumption is usually normalized to a distance of 100 km, an extrapolation is necessary due to the shorter total distance of the cycle (88 km).

$$E_{100} = \frac{E_{el}^{SOC}}{s(t_{end})}\,100 \tag{6}$$

In the current experiments, the vehicles had an average energy consumption of 20.31 kWh/100km for the baseline, respectively 19.85 kWh/100km (-2.2%) for the modified vehicle.

4. CONCLUSION

This article shows some real driving tests with two battery electric sport utility vehicles. One of them is still in series state with unmodified drivetrain and braking system, while the second vehicle is equipped with innovative chassis actuators such as In-Wheel Machines and Brake-by-Wire. In addition, the modified vehicle is controlled by new vehicle dynamics and energy management control system. During test drives in an RDE driving cycle, the differences between the vehicles were figured out, evaluated and discussed. It was found that the regenerative braking system has a remarkable impact on the power balance and range of the vehicles. In addition, the electric machines in the series production vehicle are able to decelerate the vehicle solely up to 0.3g. In the modified vehicle, the performance was worse because the friction brakes were used more frequently due to the blending controller used. Nevertheless, the in-wheel propulsion showed their high potential for improved energy efficiency, since

the results are already promising even that the controller is not perfectly tuned.

Investigating the power balance, a total amount of 3.93 kWh was recovered during the cycle. Compared to the results in (13), this is an improvement 219.5%. Future publications will describe further experiments on torque blending strategy and control based on the foundation research presented in this article, as the experiments have already demonstrated feasibility of innovative chassis components for use in the next generation of BEVs.

Apart from the obtained results and the positive outcomes of the experiments in this article, some remarks are necessary. Despite all the preparation and care taken, there are uncontrollable factors and constraints, such as traffic in the surrounding area, which can vary greatly throughout the day. To eliminate these factors, more trips at different times of the day are needed. In addition, the results were derived from a small number of trips with only two drivers. For the statistics, the number of test drives must be increased too.

Another point is the use of the SOC signal for evaluation of the energy efficiency. Due to the limitations that come with this parameter, it is less precise than using the direct traction battery signals. Therefore, a re-evaluation shall take place, as soon as the access to the battery CAN is enabled in the baseline vehicle.

Considering these points, the authors expect further improvements. As stated earlier, these points are outlined for future research in this area.

ACKNOWLEDGMENTS

The research leading to these results was funded by the European Union under the Horizon 2020 (H2020) Research and Innovation Programme (Grant Agreement No. 824250).

REFERENCES

(1) R. Irle, EV-Volumes - The Electric Vehicle World Sales Database. URL: https://www.ev-volumes.com/ (23/03/2023).

(2) J. A. Sanguesa, V. Torres-Sanz, P. Garrido, F. J. Martinez, and J. M. Marquez-Barja, "A Review on Electric Vehicles: Technologies and Challenges," *Smart Cities*, vol. 4(1), pp. 372–404, 2021.

(3) A. Nordelöf et al. "Environmental impacts of hybrid, plug-in hybrid, and battery electric vehicles—what can we learn from life cycle assessment?", *The International Journal of Life Cycle Assessment*, vol. 19(11), 2014

(4) G. Zheng & Z. Peng "Life Cycle Assessment (LCA) of BEV's environmental benefits for meeting the challenge of ICExit (Internal Combustion Engine Exit)", *Energy Reports*, vol. 7, pp. 1203 – 1213, 2021.

(5) "Electric has gone AUDI", URL: https://electrichasgoneaudi.net/models/e-tron/drivetrain/ (23/03/2023).

(6) C. Hamatschek et al. "Investigations on recuperation and operation strategies of a battery electric vehicle under real world conditions as a basis for future brake wear particle emission measurements", *EuroBrake 2022*, 2022.

(7) S. Gramstat et al. "Report on vehicle and component specifications", project interim report, 2019. URL: https://cordis.europa.eu/project/id/824250/results (23/03/2023)

(8) M. Heydrich et al. "Robust Design of combined control strategy for electric vehicle with in-wheel propulsion", IEEE Vehicle Power and Propulsion Conference (VPPC), 2020.

(9) M. Heydrich et al. "Integrated Braking Control for Electric Vehicles with In-Wheel Propulsion and Fully Decoupled Brake-by-Wire System", *Vehicles*, vol. 3(2), pp. 145-161, 2021.

(10) M. Heydrich et al. "Hardware-in-the-Loop Testing of a Hybrid Brake-by-Wire System for Electric Vehicles," *SAE Int. J. Veh. Dyn., Stab., and NVH*, vol. 6(4), 2022.

(11) AUDI AG "Antrieb. Rekuperation", *Audi MediaCenter*, URL: https://www.audi-mediacenter.com/de/audi-technik-lexikon-7180/antrieb-7227 (accessed: Mar. 23 2023).

(12) V. Ivanov et al. "Brake Blending Design Using Distributed and Shared X-in-the-Loop Test Environment", *IEEE Conference on Vehicle Power and Propulsion* (*VPPC*), 2022.

(13) AUDI AG "Fahrwerk. Elektrohydraulisch integriertes Bremsregelsystem", *Audi MediaCenter*, URL: https://www.audi-mediacenter.com/de/audi-technik-lexikon-7180/fahrwerk-7185 (accessed: Mar. 23 2023).

(14) S. Gramstat "Evaluation and testing report for the AUDI and JAC vehicles", project interim report, 2022. URL: https://cordis.europa.eu/project/id/824250/results (23/03/2023)